HHS Public Access

Author manuscript

J Cell Biochem. Author manuscript; available in PMC 2018 December 01.

Published in final edited form as:

J Cell Biochem. 2017 December ; 118(12): 4240–4253. doi:10.1002/jcb.26074.

Deletion of a Distal *RANKL* Gene Enhancer Delays Progression of Atherosclerotic Plaque Calcification in Hypercholesterolemic Mice

Sohel Shamsuzzaman[1,2], **Melda Onal**[1], **Hillary C. St John**[1,3], and **J. Wesley Pike**[1,4]

[1]Department of Biochemistry, University of Wisconsin-Madison, Madison, WI 53706, U.S.A

Abstract

Receptor activator of NF-κB ligand (RANKL) is a TNFα-like cytokine which mediates diverse physiological functions including bone remodeling and immune regulation. RANKL has been identified in atherosclerotic lesions; however, its role in atherosclerotic plaque development remains elusive. An enhancer located 75kb upstream of the murine *RANKL* gene's transcription start site designated D5 is important for its calciotropic hormone- and cytokine-mediated expression. Here, we determined the impact of RANKL levels in atherosclerotic plaque development in the D5 enhancer-null ($D5^{-/-}$) mice in an atherogenic $Apoe^{-/-}$ background fed a high-fat diet (HFD). *RANKL* mRNA transcripts were increased in aortic arches and thoracic aortae of $Apoe^{-/-}$ mice; however, this increase was blunted in $Apoe^{-/-};D5^{-/-}$ mice. Similarly, higher *RANKL* transcripts were identified in splenic T lymphocytes in $Apoe^{-/-}$ mice, and their levels were reduced in $Apoe^{-/-};D5^{-/-}$ mice. When analyzed by micro-computed tomography (μCT), atherosclerotic plaque calcification was identified in 6 out of 8 $Apoe^{-/-}$ mice, whereas only 1 out of 8 $Apoe^{-/-};D5^{-/-}$ mice developed plaque calcification after 12 weeks of HFD. However, following 18 weeks of HFD challenge, all of $Apoe^{-/-}$ and $Apoe^{-/-};D5^{-/-}$ animals developed atherosclerotic plaque calcification. Likewise, atherosclerotic lesion sizes were site-specifically reduced in the aortic arch of $Apoe^{-/-};D5^{-/-}$ mice at initial stage of atherosclerosis and this effect was diminished as atherosclerosis proceeded to a more advanced stage. Our data suggest that deletion of the *RANKL* D5 enhancer delays the progression of atherosclerotic plaque development and plaque calcification in hypercholesterolemic mice. This work provides important insight into RANKL's regulatory role in atherosclerosis.

Keywords

RANKL; distal enhancer; atherosclerotic plaque; μCT; plaque calcification; gene regulation; plaque RANKL

[4]Please send correspondence to: Professor J. Wesley Pike, Department of Biochemistry, University of Wisconsin-Madison, Hector F. DeLuca Biochemistry Laboratories, Room 543D, 433 Babcock Drive, Madison, WI 53706. Phone (608) 262-8229; Fax (608) 263-7609; pike@biochem.wisc.edu.

[2]Current address: University of Dhaka, Department of Biochemistry and Molecular Biology, Dhaka 1000, Bangladesh

[3]Current address: Cystic Fibrosis Foundation Therapeutics, Inc., 44 Hartwell Ave. Lexington, MA 02421

Disclosure Statement: The authors have nothing to disclose.

INTRODUCTION

Atherosclerosis is the leading cause of death due to cardiovascular complications in the Western nations [Collaborators, 2015; Glass and Witztum, 2001; Roth et al., 2015]. A hallmark of atherosclerosis is calcification within the plaques that arise in the blood vessel walls [Doherty et al., 2003; Thompson and Towler, 2012]. Calcified plaques have been documented in both humans and experimental models of atherosclerosis [Dhore et al., 2001; Schoppet et al., 2004], and the calcification process in the vessels has been suggested to be similar to that of endochondral bone formation [Doherty et al., 2003; Hunt et al., 2002; Mohler, 2000]. Atherosclerosis manifests a chronic inflammatory disease process [Glass and Witztum, 2001; Hansson, 2005; Libby, 2002; Libby, 2013; Ross, 1999]. Its prevalence has frequently been observed in inflammatory diseases, such as aging [London, 2011a], osteoporosis [Glass and Witztum, 2001; Hofbauer and Schoppet, 2001; Khosla, 2011; Kiel et al., 2001], hyperlipidemia [Sage et al., 2010] and end-stage renal disease [Giachelli, 2004; Giachelli, 2009; Towler, 2004]. Multiple factors including pro-inflammatory cytokines, hyperlipidemia, hyperphosphatemia and hypercalcemia trigger an osteochondrogenic response in vascular smooth muscle cells (VSMCs), enriched in the tunica media of the vessel walls [Giachelli, 2004; Giachelli, 2009; Hsu et al., 2008; Sage et al., 2010; Shanahan et al., 2011; Shroff and Shanahan, 2007; Thompson and Towler, 2012]. The phenotypically altered VSMCs deposit extracellular matrix in atherosclerotic plaques that eventually calcify [Alexander and Owens, 2012; Giachelli, 2004; Shanahan et al., 2011]. Pro-inflammatory cytokines activate catalytic proteins, mostly matrix metalloproteinases (MMPs) in macrophages that degrade extracellular matrix proteins such as collagen and also inhibit interstitial collagen synthesis in VSMCs [Hansson, 2005; Libby, 2013]. These changes ultimately cause thinning of the collagen-rich fibrous cap that covers the necrotic core of atherosclerotic plaques, and thereby rendering them prone to rupture causing thrombosis [Hansson, 2005; Libby, 2002; Libby, 2013; Libby et al., 2011; Ross, 1999].

Receptor activator of NF-κB ligand (RANKL) (encoded by *Tnfsf11* gene) is a TNFα-like cytokine that mediates diverse biological functions, primarily bone remodeling [Kong et al., 1999a; Lacey et al., 1998]; however, it is also important for other physiological processes such as lymphogenesis [Hess et al., 2012; Kong et al., 1999b], mammary gland development [Fata et al., 2000], T and B lymphopoiesis [Anderson et al., 1997; Kong et al., 1999b], dendritic cell function [Anderson et al., 1997; Loser et al., 2006] and thermoregulation [Hanada et al., 2009]. In the late 1990's, the important discovery was made that RANKL is necessary for osteoclastogenesis, and that its soluble decoy receptor, osteoprotegerin (OPG) is essential for regulating the availability of RANKL [Kong et al., 1999a; Kong et al., 1999b; Lacey et al., 1998; Simonet et al., 1997; Suda et al., 1992; Teitelbaum, 2000]. RANKL exerts its actions via binding to its cognate receptor, RANK [Anderson et al., 1997; Dougall et al., 1999] which is highly expressed in hematopoietic precursors of the monocyte/macrophage-lineage cells that ultimately become bone-resorbing osteoclasts [Boyle et al., 2003; Lacey et al., 1998; Teitelbaum, 2000]. In many physiological conditions that demand release of calcium from the skeletal stores, such as lactation, modulation of RANKL and OPG levels is one of the main mechanisms that is utilized to increase bone resorption [Ardeshirpour et al., 2010; Ardeshirpour et al., 2015]. However, many pathological

conditions, such as secondary hyperparathyroidism, lead to an imbalance in RANKL and OPG levels leading to either osteoporosis or osteopetrosis, underscoring the importance of exquisite fine tuning of RANKL and OPG's levels [Bucay et al., 1998; Hofbauer and Schoppet, 2001; Hofbauer and Schoppet, 2004; Sobacchi et al., 2007]. The RANK:RANKL:OPG triad, critical for bone remodeling is also evident in the vascular system [Collin-Osdoby, 2004; Dhore et al., 2001; Papadopouli et al., 2008; Quercioli et al., 2010; Sandberg et al., 2006; Schoppet et al., 2004; Tintut and Demer, 2006]. Bone remodeling components are documented in both human and experimental cases of vascular calcification [Choi et al., 2008; Dhore et al., 2001; Hunt et al., 2002; Kaden et al., 2004; Min et al., 2000; Mohler, 2000; Ndip et al., 2011; Osako et al., 2010]. Studies over the past decade have established that ectopic calcification in the vasculature follows a process similar to endochondral ossification and have suggested an involvement of the RANK:RANKL:OPG triad in atherosclerosis [Bennett et al., 2006; Dhore et al., 2001; Helas et al., 2009; Kiechl et al., 2007; Panizo et al., 2009; Sandberg et al., 2006; Schoppet et al., 2004].

Bone regulating factors such as parathyroid hormone (PTH), 1,25-dihydroxyvitamin D_3 ($1,25(OH)_2D_3$) and interleukin (IL)-6 type cytokines modulate RANKL expression [O'Brien, 2010]. Given the diverse source of RANKL in stromal cells/osteoblasts [Yasuda et al., 1998], T and B lymphocytes [Anderson et al., 1997; Kanematsu et al., 2000; Wong et al., 1997], osteocytes [Xiong et al., 2011], keratinocytes [Loser et al., 2006], synovial fibroblasts [Danks et al., 2015], vascular endothelial cells [Collin-Osdoby et al., 2001], vascular smooth muscle cells (VSMCs) [Byon et al., 2011; Di Bartolo et al., 2013; Sun et al., 2012; Tseng et al., 2010], and its regulation by various factors, RANKL is poised to be a critical molecule at the interface of the bone-vascular axis. Since RANKL has emerged as an important regulatory factor not only for bone remodeling, but also is associated with multiple pathologic states [Guerrini and Takayanagi, 2014; Hofbauer and Schoppet, 2001], intense efforts over the past several years have been made to elucidate RANKL's regulatory landscape at the genomic level [Bishop et al., 2011; Bishop et al., 2009; Bishop et al., 2015; Fu et al., 2006; Galli et al., 2008; Kim et al., 2006; Nerenz et al., 2008]. Via genome-wide ChIP-sequencing approaches, we have discovered ten RANKL distal enhancers, spanning over 200 kb upstream of both murine and human RANKL gene's transcription start site (TSS) [Bishop et al., 2011; Bishop et al., 2009; Bishop et al., 2015; Galli et al., 2008; Kim et al., 2006; Nerenz et al., 2008]. Subsequently, we have conducted comprehensive *in vivo* analyses of some of the RANKL distal enhancers in murine model [Galli et al., 2008; Onal et al., 2014b; Onal et al., 2015]. Of particular interest, deletion of the multi-lineage multifunctional D5 enhancer of RANKL, located 75 upstream of *RANKL* gene's TSS, leads to reduced basal RANKL levels in bones and lymphoid tissues [Galli et al., 2008]. Accordingly, D5 enhancer-null ($D5^{-/-}$) mice display increased bone mass due to reduced rate of bone remodeling [Galli et al., 2008]. As previously mentioned, RANKL has been identified in atherosclerotic plaques in both humans and animal models [Byon et al., 2011; Dhore et al., 2001; Osako et al., 2010; Schoppet et al., 2004; Sun et al., 2012]. Although, some studies have shown that exogenous RANKL could enhance calcification in vascular smooth muscle cells [Osako et al., 2010; Panizo et al., 2009], others have not [Byon et al., 2011; Morony et al., 2012; Olesen et al., 2012; Tseng et al., 2010], and direct *in vivo*

evidence of RANKL's role in atherosclerotic plaque development remains lacking. In our present study, we explored the impact of reduced basal RANKL levels in atherosclerotic plaque formation in the D5 enhancer-null ($D5^{-/-}$) mouse model in an atherogenic $Apoe^{-/-}$ background. Here, we show that deletion of the RANKL *D5* enhancer delays the progression of atherosclerotic plaque development and plaque calcification in hypercholesterolemic *Apoe*-null mice.

MATERIALS AND METHODS

Animal Studies

The *Apoe*-null ($Apoe^{-/-}$) mice in the C57BL/6 background were purchased from the Jackson Laboratory (Bar Harbor, ME; Cat. No. 002052). The $D5^{-/-}$ mice has been extensively studies and kindly provided by O'Brien *et al* [Galli et al., 2008; Onal et al., 2012; Onal et al., 2016b]. The $Rankl^{-/-}$ [Kim et al., 2000] and $Rankl^{-/-;Tg}$ transgenic mice [Onal et al., 2014a] in the C57BL/6 background have been described previously. The $Apoe^{-/-}$ mice were crossed with the $D5^{-/-}$ mice to generate the $Apoe^{-/-}$;$D5^{-/-}$ mice. Only female mice were used for this study. Upon weaning mice were placed on a low fat control diet (Harlan Teklad, Madison, WI; TD.08485) up to start of the study. In the beginning of the study, all mice at 7 weeks of age were placed on a high-fat diet (HFD) (Harlan Teklad, Madison, WI; TD.88137) for a further 12 or 18 weeks to promote atherosclerosis. All animal studies were reviewed and approved by the University of Wisconsin-Madison Animal Care and Use Committee.

Serum and Plasma Analysis

Blood was collected at the time of sacrifice by cardiac puncture, following 4 hours (h) of fasting. Serum calcium (BioAssay Systems; Cat. No. DICA-500) and phosphate (BioAssay Systems; Cat. No. DIPI-500), and plasma parathyroid hormone (PTH) (Immutopics; Cat. No. 60-2305) levels were determined as described previously [Lee et al., 2014; Shamsuzzaman et al., 2016]. The serum total cholesterol, LDL-cholesterol and HDL-cholesterol were measured using Cholesterol E (Cat. No. 439-17501), L-type LDL-C (Cat. No. 993-00404 and 999-00504) and HDL-Cholesterol (Cat. No. 431-52501) kits, respectively (Wako Chemicals USA, Richmond, VA). The serum triglyceride (TG) concentration was measured as previously described using the Infinity^{TM} Triglycerides (Cat. No. TR22421,Thermo Scientific, Middletown, VA) [Shamsuzzaman et al., 2016].

Bone Mineral Density (BMD) Measurements

BMD was measured and analyzed by dual-energy X-ray absorptiometry (DEXA) scans using a PIXImus densitometer (GE-Lunar, Madison, WI) as described previously [Onal et al., 2014a; Onal et al., 2016b]. BMD was performed following either 12 or 18 weeks of high-fat diet (HFD) feeding.

Micro-computed Tomography (μCT) Analysis

Animals were euthanized by using CO_2 asphyxiation. Immediately after euthanasia, mice were perfused with cold sterile PBS followed by 4% paraformaldehyde solution. Excised heart and aorta specimens were fixed in 10% Millonig's Modified Buffered Formalin (Leica

Biosystems, Richmond, IL) for 72 h at 4°C. Following fixation, specimens were washed in PBS with 0.02% sodium azide for 24 h. μCT analysis of the aortas were done as previously described [Shamsuzzaman et al., 2016]. Briefly, immediately prior to μCT scanning, aortae were perfused with corn oil via injection and immersed in corn oil during the scan. All samples were scanned with a Siemens microCATII scanner (Siemens Medical Solutions USA, Inc., Knoxville, TN) with the following parameters: 5 second exposure time, binning factor 1, 55 kVp, 50 μA, 220 rotation steps and 440 projections. The final reconstructed isotropic voxels were 34 μm. Inveon Research Workplace 3D Visualization analysis software (Siemens Medical Solutions USA, Inc., Knoxville, TN) was used to provide qualitative graphics and to measure calcified plaque volume, surface area, and density. Segmentation of calcified plaque was defined by voxels with an HU value greater than 325 (previously determined threshold to exclude cartilaginous or fibrous tissue and include all calcified plaque) [Shamsuzzaman et al., 2016].

Atherosclerotic Lesion Analysis

For histological analysis, sections (10-μm thick) were prepared from the aortic root, aortic arch, innominate artery and thoracic aorta. Atherosclerotic lesions in aortic roots were analyzed by oil red O staining throughout 300 μm of aortic sinus region starting at the aortic valve leaflets. Mean lesion area was quantified from digitally captured 5 sections separated by 60 μm using ImageJ software (NIH, Bethesda, MD). For measurement of atherosclerotic lesions in aortic arch, innominate artery and thoracic aorta, tissues were sectioned longitudinally and mean lesion area was quantified from 5 sections over a 100 μm region. The calcium deposition in the atherosclerotic lesions was identified by von Kossa staining using kit according to manufacturer's instructions (American Mastertech Scientific, Inc. Lodi, CA; Cat. No. KTVKO).

Gene Expression Analysis

Upon isolation from the mouse the aortas were placed in and cleaned in RNA*later* RNA Stabilization Reagent (Qiagen Inc., Valencia, CA; Cat. No. 76104), total RNA was prepared from the aortic arch and the thoracic aorta using RNeasy Fibrous Tissue Mini Kit (Qiagen Inc., Valencia, CA; Cat. No. 74704) according to manufacturer's protocol. Other tissues were homogenized in Trizol Reagent (Life Technologies, Grand Island, NY; Cat. No. 15596018) and RNA was isolated according to manufacturer's protocols. One microgram of total RNA was used to prepare cDNA using High Capacity cDNA Reverse Transcription kit (Applied Biosystems, Foster City, CA; Cat. No. 4368813). Relative mRNA levels were measured by TaqMan qRT-PCR as described previously [Onal et al., 2014a]. The following TaqMan gene expression probes (Applied Biosystems, Foster City, CA) were used for qRT-PCR: *Rankl* (*Tnfsf11*, Mm00441906_m1), *Opg* (*Tnfrsf11b*, Mm01205928_m1), *Rank* (*Tnfrsf11a*, Mm00437135_m1), *Runx2* (Mm00501584_m1), *Alpl* (Mm00475834_m1), *Opn (Spp1,* Mm00436767_m1), *Sp7* (Mm04209856_m1), *Enpp1* (Mm00501097_m1), *Enpp3* (Mm01193731_m1), *Mmp13* (Mm00439491_m1), *Il-6* (Mm00446190_m1), *Tnf-α (*Mm00443258_m1), *Lgr4* (Mm00554385_m1), and β-actin (*Actb*, 4352341E).

In vivo Isolation of T and B Lymphocytes

Total T and B lymphocytes were isolated from the spleens and bone marrow (BM) using mouse Dynabeads Mouse Pan T (Thy1.2 Cat. No. 11443D) and Dynabeads Mouse pan B (B220; Cat. No. 11441D) kits according to manufacturer's instructions (Life Technologies, Grand Island, NY). The RNA from isolated T and B lymphocytes was prepared using Trizol Reagent (Life Technologies, Grand Island, NY). One μg of the isolated RNA was DNase treated and reverse transcribed for RT-PCR as explained in the previous section.

Isolation and Culture of Murine Aortic Smooth Muscle Cells

The murine aortic smooth muscle cells (mAoSMCs) were isolated from thoracic aortae of WT, $D5^{-/-}$, $Rankl^{-/-}$ and $Rankl^{-/-;Tg}$ mice by enzymatic digestion with collagenase type II (255 U/mL; Worthington Biochemical Corp., Lakewood, NJ), elastase type III (15 U/mL; Sigma-Aldrich, St. Louis, MO), soybean trypsin inhibitor (375 μg/mL; Gibco) and bovine serum albumin (2 mg/mL; Jackson ImmunoResearch Laboratories Inc., West Grove, PA) as described previously [Clowes et al., 1994; Shamsuzzaman et al., 2016]. mAoSMCs were cultured in DMEM modified to contain 1 g/L D-glucose, GlutaMAX, 110 mg/L sodium pyruvate supplemented with 10% fetal bovine serum (Hyclone, Logan, UT) and 1% penicillin/streptomycin (Hyclone, Logan, UT). Cells between three and seven passages were grown to confluency in standard media (SM) as mentioned above and then switched to osteogenic medium (OM, SM supplemented with 10 mM β-glycerophosphate, 50 μg/mL ascorbic acid and 100 nM dexamethasone) for additional 21 days. Alizarin red S staining was performed as described previously [Meyer et al., 2014]. Von Kossa staining was performed by using kit according to manufacturer's instructions (American Mastertech Scientific, Inc. Lodi, CA; Cat. No. KTVKO). For calcium assay, cells were decalcified with 0.6 N HCl at 4°C for 24 h. Calcium content was measured by using O-cresolphthalein complexone method (Sigma-Aldrich, St. Louis, MO; Cat. No. MAK022-1KT) and normalized to total protein content of decalcified cells.

Statistical Analysis

All data were analyzed using GraphPad Prism 4 software (GraphPad Software, Inc., La Jolla, CA). Data are presented as mean ± standard error of the mean (s.e.m). Statistical significance was determined by one-way analysis of variance (ANOVA) with Tukey's test for multiple groups or by nonparametric Student's *t*-test for two groups. $P < 0.05$ was considered to be statistically significant.

RESULTS

Deletion of the *RANKL* D5 enhancer reduces matrix calcification in murine aortic smooth muscle cells

To evaluate potential transdifferentiation and calcium deposition abilities *in vitro*, we isolated primary murine aortic smooth muscle cells mAoSMCs from wild-type (WT), *Rankl*-null ($Rankl^{-/-}$), *Rankl* transgenic rescue ($Rankl^{-/-;Tg}$) and D5 enhancer-null ($D5^{-/-}$) mice. We cultured mAoSMCs in the presence of a high-phosphate osteogenic medium (OM) for 21 days to differentiate them into osteoblast-like cells. As can be seen in Fig. 1a, WT

mAoSMCs developed substantial matrix calcification as evident by both alizarin red S and von Kossa staining. On the contrary, the *Rankl*$^{-/-}$ mAoSMCs produced less matrix calcification compared to WT mAoSMCs. However, when RANKL was expressed exogenously by a transgene in *Rankl*$^{-/-}$ background, the *Rankl*$^{-/-;Tg}$ mAoSMCs recovered their matrix forming and calcification potentials (Fig. 1a). Interestingly, the mAoSMCs that lack RANKL's D5 enhancer (*D5*$^{-/-}$) displayed significantly less matrix calcification compared to WTs as well (Fig. 1a). Quantification of calcium content after decalcifying the cells confirmed the observations made in alizarin red and von Kossa staining (Fig. 1b). These results suggest that endogenous expression of RANKL, specifically its D5 mediated-expression, plays a role in calcium deposition of mAoSMCs differentiated into osteogenic cells.

Deletion of the *RANKL* D5 enhancer does not alter serum lipid and mineral homeostasis in hypercholesterolemic *Apoe*$^{-/-}$ background

Apoe$^{-/-}$ mice develop severe hypercholesterolemia when fed a high-fat diet (HFD) [Plump et al., 1992]. To assess the impact of lack of the *RANKL* D5 enhancer in mice in an *Apoe*$^{-/-}$ background, we analyzed their serum lipid profiles after feeding the HFD for either 12 or 18 weeks. *WT* and *D5*$^{-/-}$ mice maintained normal serum lipid levels after HFD feeding (Supplementary Fig. 1a–h). *Apoe*$^{-/-}$ mice developed marked hypercholesterolemia as seen by their high serum triglyceride (TG), total cholesterol and LDL-cholesterol (LDL-C) levels, however, low HDL-cholesterol (HDL-C) level (Supplementary Fig. 1a–h). Likewise, *Apoe*$^{-/-}$*;D5*$^{-/-}$ mice also displayed marked hypercholesterolemia, and all the lipid parameters were comparable with *Apoe*$^{-/-}$ mice. In addition, both *Apoe*$^{-/-}$ mice also developed hypercalcemia and hyperphosphatemia when fed the HFD (Supplementary Fig. 1i–l). Therefore, lack of *RANKL* D5 does not alter serum lipid and mineral homeostasis in mice in an *Apoe*-null background.

Deletion of the *RANKL* D5 enhancer leads to increased bone mass in the *Apoe*$^{-/-}$ background

Lack of the *RANKL* D5 enhancer leads to bone mass accrual in mice due to reduced rate of bone remodeling [Galli et al., 2008]. We therefore first determined whether the lack of the D5 enhancer altered bone mass in our mouse model of atherosclerosis in an *Apoe*$^{-/-}$ background. *D5*$^{-/-}$ mice exhibited higher bone mineral density (BMD) globally as well as in the spine and the femur compared to *WT* control littermates, which confirms previous observations made by Galli and colleagues [Galli et al., 2008] (Fig. 2a–f). Consistent with the role of D5-mediated regulation of RANKL expression in bone, the absence of the D5 enhancer lead to elevated vertebral and whole body BMD of *Apoe*$^{-/-}$*;D5*$^{-/-}$ mice after feeding the HFD either for 12 or 18 weeks (Fig. 2a–f). Surprisingly, *Apoe*$^{-/-}$mice maintained comparable or higher BMD than *WT* littermate controls after feeding the HFD (Fig. 2a–f). Accordingly, the *Rankl* mRNA transcripts were lower in the tibiae and lymphoid tissues of both *D5*$^{-/-}$ and *Apo*$^{-/-}$*;D5*$^{-/-}$ mice (Fig. 2g–i). Interestingly, compared to *WT* and *D5*$^{-/-}$ mice, mice in the *Apoe*-null background had lower *Opg* mRNA levels in tibia, but not lymphoid tissues (Fig. 2j–l). These results demonstrate that a decrease in RANKL levels due to the lack of RANKL D5 enhancer caused a high bone mass phenotype and this effect was not altered in mice in an atherogenic *Apoe*-null background.

Deletion of the D5 enhancer decreases RANKL expression in atherosclerotic lesions

To determine RANKL levels and its regulation by the D5 enhancer in atherosclerotic lesions, we isolated RNA from the aortic arches and the thoracic aortae of mice fed the HFD for 18 weeks (Fig. 3a) and then examined the expression of *Rankl* mRNA transcripts. *Rankl* transcripts were greater in the aortic arches and the thoracic aortae of both $Apoe^{-/-}$ and $Apoe^{-/-};D5^{-/-}$ mice fed the HFD for 18 weeks compared to *WT* or $D5^{-/-}$ littermate controls (Fig. 3b). Importantly, RANKL mRNA levels were significantly lower in $Apoe^{-/-};D5^{-/-}$ mice compared to $Apoe^{-/-}$ mice, suggesting that D5 mediates the increase in RANKL expression in atherosclerotic lesions (Fig. 3b). *Opg* mRNA transcripts were equally elevated in aortae of both $Apoe^{-/-}$ and $Apoe^{-/-};D5^{-/-}$ mice (Fig. 3c). *Lgr4*, a recently identified novel receptor for RANKL [Luo et al., 2016], was significantly decreased in both aortic arch and the thoracic aorta of $Apoe^{-/-};D5^{-/-}$ mice as compared to $Apoe^{-/-}$ mice as well as *WT* and $D5^{-/-}$ controls (Fig. 3d). The expression of the classic RANKL receptor, *Rank* was decreased in aortic arches of both $Apoe^{-/-}$ and $Apoe^{-/-};D5^{-/-}$ mice as compared to *WT* littermate controls (Fig. 3e). These results demonstrate that RANKL expression is induced in a D5-dependent manner in atherosclerotic lesions of hypercholesterolemic *Apoe*-null mice.

Inflammatory and osteogenic responses are modified in hypercholesterolemic mice

Next, we examined whether the expression of key inflammatory and osteogenic markers was affected by lower RANKL levels in the aortae of $Apoe^{-/-};D5^{-/-}$ mice after feeding the HFD for 18 weeks. mRNA transcripts of pro-inflammatory genes, interleukin-6 (*Il-6)* and tumor necrosis factor-α (*Tnf-α)* were elevated similarly in both $Apoe^{-/-}$ and $Apoe^{-/-};D5^{-/-}$ aortae as compared to littermate controls (Fig. 4a,b). In addition, osteogenic markers representing the degree of osteogenic potential and bone formation, *Runx2*, *Sp7*, *Opn* and *Alpl* were induced similarly in aortae isolated from the $Apoe^{-/-}$ and $Apoe^{-/-};D5^{-/-}$ mice compared to controls (Fig. 4c–f). These results demonstrate that expression of the key inflammatory and osteogenic regulators are locally modulated in atherosclerotic lesions of both $Apoe^{-/-}$ and $Apoe^{-/-};D5^{-/-}$ mice, and are not affected by the blunting of the increase in atherosclerotic plaque RANKL in $Apoe^{-/-};D5^{-/-}$ mice.

Lack of D5 blunts the atherosclerosis-induced increase in T cell RANKL

Lymphocytes are an important source of RANKL [Anderson et al., 1997; Kanematsu et al., 2000; Wong et al., 1997]. We sought to determine the relative contributions of T and B lymphocytes to RANKL levels in our mouse model of atherosclerosis. We isolated total $CD3^+$ T and $B220^+$ B lymphocytes from the spleens of *WT*, $D5^{-/-}$, $Apoe^{-/-}$ and $Apoe^{-/-};D5^{-/-}$ mice fed the HFD, and assessed *Rankl* mRNA transcripts in these cells. Consistent with our previous studies [Onal et al., 2016a], lack of D5 led to lower *Rankl* mRNA levels in T lymphocytes isolated from the $D5^{-/-}$ and $Apoe^{-/-};D5^{-/-}$ mice as compared to *WT* littermate controls after 12 weeks of HFD feeding (Fig. 5a). Interestingly, after 18 weeks of HFD feeding *Rankl* mRNA transcripts were elevated in splenic T lymphocytes of $Apoe^{-/-}$ mice as compared to *WT* controls and this increase was prevented by the lack of D5 regulation of RANKL in $Apoe^{-/-};D5^{-/-}$ mice (Fig. 5a). Basal levels of *Rankl* mRNA transcripts were also lower in B lymphocytes (Fig. 5a). *Rankl* transcripts in B

lymphocytes were similarly reduced in both *D5*$^{-/-}$ and *Apoe*$^{-/-}$;*D5*$^{-/-}$ mice after initial 12 weeks of HFD feeding, however, we were unable to detect this small difference after 18 weeks of HFD challenge (Fig. 5a). The splenic weights were similarly increased in both *Apoe*$^{-/-}$ and *Apoe*$^{-/-}$;*D5*$^{-/-}$ mice fed the HFD for 18 weeks, suggesting an elevated inflammation in mice in the *Apoe*-null background (Fig. 5b). Next, we examined the expression of key inflammatory genes in the splenic T lymphocytes of mice after feeding the HFD for either 12 or 18 weeks. Pro-inflammatory cytokine *Tnf-α* mRNA was elevated in T lymphocytes of *Apoe*$^{-/-}$, but not *Apoe*$^{-/-}$;*D5*$^{-/-}$, mice after initial 12 weeks of HFD feeding (Fig. 5c), however this effect was blunted after 18 weeks of HFD feeding. Similarly, monocyte chemoattractant peptide-1 (*Mcp-1*) mRNA, elevated in T lymphocytes of *Apoe*$^{-/-}$ mice, was unaffected in *Apoe*$^{-/-}$;*D5*$^{-/-}$ mice after 12 weeks of HFD; again there was no difference between the two genotypes after 18 weeks of HFD (Fig. 5d). mRNA levels for Interferon γ (*Ifn-γ*), a signature T helper type 1 (T_H1) cytokine, were equally elevated in T lymphocytes of *Apoe*$^{-/-}$ and *Apoe*$^{-/-}$;*D5*$^{-/-}$ mice after 18 weeks of HFD feeding only (Fig. 5e). These results suggest that T cell RANKL is elevated via D5 mediated regulation in atherosclerotic mice and that lower RANKL levels in *Apoe*$^{-/-}$;*D5*$^{-/-}$ mice lead to lower pro-inflammatory responses at an early stage of atherosclerosis.

Deletion of the RANKL D5 enhancer in the *Apoe*$^{-/-}$ background delays progression of atherosclerotic plaque calcification

Atherosclerotic plaques become calcified as the disease advances progressively [Dhore et al., 2001; Doherty et al., 2003; Schoppet et al., 2004; Thompson and Towler, 2012]. To determine if the blunted-increase in atherosclerotic plaque RANKL in *Apoe*$^{-/-}$;*D5*$^{-/-}$ mice affects the calcification of atherosclerotic plaques, we employed micro-computed tomography (μCT) to assess the total calcified plaque burdens in the aortae after feeding mice the HFD for either 12 or 18 weeks. No atherosclerotic lesions or plaque calcification were observed in *WT* or *D5*$^{-/-}$ mice after either 12 or 18 weeks of HFD feeding (Fig. 6a–f and Table). When analyzed by μCT, 6 out of 8 *Apoe*$^{-/-}$ mice (75%) developed atherosclerotic plaque calcification after 12 weeks of HFD feeding, whereas, only 1 out of 8 *Apoe*$^{-/-}$;*D5*$^{-/-}$ mice developed plaque calcification (Fig. 6a–d and Table) after initial 12 weeks of HFD. Surprisingly, after 18 weeks of HDF challenge, 100% of both the *Apoe*$^{-/-}$ and *Apoe*$^{-/-}$;*D5*$^{-/-}$ mice developed atherosclerotic plaque calcification (Fig 6a–d and Table). Likewise, atherosclerotic lesion size was reduced by 34.7% in the aortic arch (AA) in *Apoe*$^{-/-}$;*D5*$^{-/-}$ as compared to *Apoe*$^{-/-}$ after 12 weeks of HFD feeding, although lesion sizes remained unchanged in other atherosclerosis-prone sites e.g., aortic root (AR), innominate artery (IA) and thoracic aorta (TA) in either genotype (Fig. 6e). Interestingly, after 18 weeks of HFD feeding the atherosclerotic lesion sizes were indistinguishable at all sites between *Apoe*$^{-/-}$;*D5*$^{-/-}$ and *Apoe*$^{-/-}$ mice (Fig. 6f). As can be seen in Fig. 6 c–d, the calcified plaque surface area and plaque volume were increased gradually over time in *Apoe*$^{-/-}$ as well as in *Apoe*$^{-/-}$;*D5*$^{-/-}$ mice. Taken together, our data show that deletion of the *RANKL* D5 enhancer delays the progression of the atherosclerotic plaque formation and plaque calcification in hypercholesterolemic *Apoe*-null background.

DISCUSSION

RANKL mediates inflammatory responses primarily via nuclear factor κB (NF-κB) signaling. Although initially discovered as the key osteoclastogenic factor [Kim et al., 2000; Kong et al., 1999b; Lacey et al., 1998], studies over the past decade have unraveled a wide range of biological functions of RANKL [Anderson et al., 1997; Fata et al., 2000; Hanada et al., 2009; Hess et al., 2012; Kong et al., 1999a; Loser et al., 2006], and its diverse cellular sources [Anderson et al., 1997; Byon et al., 2011; Danks et al., 2015; Di Bartolo et al., 2013; Kanematsu et al., 2000; Sun et al., 2012; Tseng et al., 2010; Wong et al., 1997; Xiong et al., 2011; Yasuda et al., 1998]. RANKL binds to RANK [Anderson et al., 1997; Dougall et al., 1999] on target cells; however, a novel receptor of RANKL, designated LGR4 has recently been reported [Luo et al., 2016]. RANKL is not only critical for bone-remodeling [Kim et al., 2000; Kong et al., 1999b] but also important for immune regulation [Anderson et al., 1997; Hess et al., 2012; Kong et al., 1999a; Loser et al., 2006], among other functions [Fata et al., 2000; Hanada et al., 2009]. Subsequently, linkage has been discovered with a wide variety of skeletal, inflammatory and non-inflammatory diseases such as osteoporosis, aging, autoimmunity, cancer and diabetes [Collin-Osdoby, 2004; Hofbauer and Schoppet, 2001; Hofbauer and Schoppet, 2004; Khosla, 2011; Kiechl et al., 2013]. Therefore, it is not surprising that RANKL is an important pharmacologic target for multiple diseases [Cummings et al., 2009; Helas et al., 2009; Hofbauer and Schoppet, 2004; Smith et al., 2009].

RANKL has also been implicated in vascular calcification [Dhore et al., 2001; Helas et al., 2009; Kaden et al., 2004; Kiechl et al., 2007; Ndip et al., 2011]. Recent *in vitro* studies have shown that RANKL may be playing a role in vascular calcification [Deuell et al., 2012; Kaden et al., 2004; Morony et al., 2012; Osako et al., 2010; Panizo et al., 2009], however, its role in atherosclerotic plaque development and plaque calcification *in vivo* is not well understood. In our current study, we determined the impact of reduced basal *RANKL* levels due to ablation of the RANKL D5 distal enhancer on atherosclerotic plaque development and plaque calcification by utilizing D5 enhancer-null ($D5^{-/-}$) mice in an $Apoe^{-/-}$ background. We showed that in addition to reducing RANKL expression in skeletal sites, lack of RANKL D5 enhancer blunted the disease-induced increase in RANKL expression in atherosclerotic plaques and T cells in the Apoe null background. Consistent with our in vitro observation that RANKL plays role in calcification abilities of differentiated mAoSMCs, the decrease in RANKL levels lead to delayed atherosclerotic plaque calcification and a decrease in atherosclerotic lesion area in aortic arches. Thus, we establish a novel role for RANKL in atherosclerotic plaque progression *in vivo*.

Vascular smooth muscle cells (VSMCs) modify their phenotype towards osteoblast-like cells in atherosclerotic plaques in response to inflammation, hyperlipidemia, oxidative stress and others [Alexander and Owens, 2012; Giachelli, 2004; Giachelli, 2009; Naik et al., 2012; Sage et al., 2010; Shao et al., 2010; Speer et al., 2009; Steitz et al., 2001; Thompson and Towler, 2012]. It has been shown that murine aortic cells overexpressing RANKL display enhanced mineralization potential [Morony et al., 2012]. Interestingly, we show herein that the $D5^{-/-}$ and $Rankl^{-/-}$ mAoSMCs displays reduced matrix calcification in response to high-phosphate osteogenic medium, supporting the idea that endogenous RANKL can mediate

calcification in vascular smooth muscle cells *in vitro* [Osako et al., 2010; Panizo et al., 2009]. To determine if RANKL levels are modulated *in vivo* and to establish the pathophysiological role of this regulation in atherosclerosis, we created an appropriate *in vivo* atherosclerosis model in which the RANKL D5 enhancer was deleted in the context of the *Apoe*$^{-/-}$ mouse. The novel finding is that the observed site-specific elevation of the atherosclerotic plaque *RANKL* in *Apoe*$^{-/-}$ mice were significantly reduced when the *RANKL* D5 enhancer was ablated in *Apoe*$^{-/-}$*;D5*$^{-/-}$ mice. We also observed increases in mRNA transcripts of the key pro-inflammatory cytokines, *IL-6* and *Tnf-α,* as well as increases in osteogenic regulators, *Runx2*, osterix (*Sp7*), osteopontin (*Spp1*) and alkaline phosphatase (*Alpl)* in both *Apoe*$^{-/-}$*;D5*$^{+/+}$ and *Apoe*$^{-/-}$*;D5*$^{-/-}$ aortae, suggesting that both the increase in local inflammation and/or increase in the osteogenic cell population could also be the cause of the increased plaque RANKL. Further studies utilizing additional enhancers of RANKL such as D6 or D2, which regulate inflammatory and mesenchymal lineage-specific expression of RANKL, respectively, will be of great value in dissecting the mechanisms through which RANKL is increased in atherosclerotic plaques themselves. Regardless of the stimulant, consistent with our in vitro observations, the blunting of the RANKL-induction resulted in delayed calcification of the atherosclerotic plaques in *Apoe*$^{-/-}$*;D5*$^{-/-}$ mice.

Atherosclerosis is a chronic inflammatory disease [Libby, 2002; Ross, 1999]. It is well-known that a T helper type 1 (T_H1) pro-inflammatory immune response is manifested in atherosclerosis [Hansson, 2005; Libby, 2002; Ross, 1999]. Accordingly, we isolated T and B lymphocytes from spleens of mice fed the HFD for either 12 or 18 weeks to assess the inflammatory status in our mouse models. The *Rankl* mRNA transcripts were reduced in splenic T and B lymphocytes in both *D5*$^{-/-}$ and *Apoe*$^{-/-}$*;D5*$^{-/-}$ mice after 12 weeks of HFD feeding. As atherosclerotic disease advanced, after 18 weeks of HFD feeding, the T lymphocytic *Rankl* transcripts were significantly elevated in *Apoe*$^{-/-}$ *mice,* likely due to increased inflammation in advanced atherosclerotic state. However, lack of D5 regulation of RANKL in T cells of *Apoe*$^{-/-}$*;D5*$^{-/-}$ mice prevented this increase. Recently, it has been shown that T cell RANKL is required for T cell trafficking in experimental autoimmune encephalomyelitis (EAE) [Guerrini et al., 2015]. Thus, prevention of the induction of T cell RANKL might have contributed to the T lymphocyte infiltration into the atherosclerotic plaques of *Apoe*$^{-/-}$*;D5*$^{-/-}$ mice in our study. Further investigation of T cell RANKL and its role in this disease will also be of great importance.

In addition to RANKL, Apoe$^{-/-}$ T cells exhibited an increase in expression of the major pro-inflammatory cytokine, *Tnf-α* and chemokine, *Mcp-1* after initial 12 weeks of HFD feeding, although this effect was not observed at the later time point of HFD feeding. These increases were not observed in *Apoe*$^{-/-}$*;D5*$^{-/-}$ mice, however, suggesting a stage-specific reduction of inflammation in these animals. Both TNF-α and MCP-1 have been shown to promote osteogenic responses in VSMCs [Al-Aly et al., 2007; Sun et al., 2012] and are associated with clinical cases of atherosclerosis in humans [Khosla, 2011; Libby, 2002; Libby et al., 2011; London, 2011b; Sandberg et al., 2006]. RANKL enhances MCP-1 release in mononuclear phagocytes [Sandberg et al., 2006], and *Mcp-1*-null mice on an *Ldlr*$^{-/-}$ background that results in decreased macrophage infiltration into the aortic walls as well as reduced lipid accumulation in atherosclerotic lesions [Gu et al., 1998]. Therefore, the

decreased *Tnf-α* and *Mcp-1* mRNA levels in T lymphocytes at the early stage of atherosclerosis in our *Apoe*$^{-/-}$;*D5*$^{-/-}$ mouse model may be due to a reduction of RANKL activity in splenic tissues and perhaps in the atherosclerotic plaques as well.

Coronary artery calcium (CAC) score is routinely used to predict future cardiovascular disease risks [McClelland et al., 2006]. Here, we assessed the impact of D5 enhancer deletion on atherosclerotic plaque calcification in mice. We utilized a μCT-based approach to quantify overall plaque-burdens in aorta, spanning the aortic root to the thoracic aorta after feeding mice the HFD. When analyzed by μCT, we discovered that while 75% of *Apoe*$^{-/-}$ mice developed atherosclerotic plaque calcification, only 1 out of 8 *Apoe*$^{-/-}$;*D5*$^{-/-}$ mice displayed plaque calcification after initial 12 weeks of HFD feeding; However, 100% of both *Apoe*$^{-/-}$ and *Apoe*$^{-/-}$;*D5*$^{-/-}$ mice developed atherosclerotic plaque calcification at the later stage. Therefore, *RANKL* D5 enhancer deletion delays the progression of atherosclerotic plaque calcification in *Apoe*$^{-/-}$;*D5*$^{-/-}$ mice as compared to *Apoe*$^{-/-}$ mice. Likewise, deletion of the D5 enhancer in *Apoe*$^{-/-}$;*D5*$^{-/-}$ mice reduced atherosclerotic lesion size in the aortic arch, but not other sites at an early stage of atherosclerotic plaque development, after 12 weeks of HFD feeding. However, this effect was blunted at an advanced stage of atherosclerosis following 18 weeks of HFD feeding. Accordingly, this site-specific reduction in atherosclerotic lesion size and calcification in the aortas of the *Apoe*$^{-/-}$;*D5*$^{-/-}$ mice could be due to direct effects of lower RANKL levels such as reduced mAoSMCs matrix formation, decreased Lrg4 signaling, T cell trafficking or secondary effects of lower RANKL levels such as reductions in pro-inflammatory T cell responses, or decreased levels of receptors for RANKL.

As can be deducted from above, there are multiple factors with the potential to mediate increased RANKL expression in the multiple cell types present in atherosclerotic plaques. The complexity of this disease and the multitude of RANKL expressing candidate cell types, makes it suboptimal to apply the classic approach to identifying RANKL's pathophysiological role in this disease by deleting the gene from the plaques in a cell-type specific manner. Moreover, while cell type specific deletion provides insight into requirement of RANKL, upregulation of the gene product cannot be tested in that setting. Thus, to determine the pathological role of the RANKL regulation in atherosclerotic plaques, we utilized ablation of a multifunctional multi-lineage enhancer in an attempt to blunt the increase in plaque RANKL expression regardless of the cell type or inducer. This approach has provided us with a novel insight into the role of RANKL in atherosclerosis. With this *in vivo* evidence, we can now determine the cell types involved in the pathophysiological processes that lead to this induction. To this end, animal models that lack cell-type or factor-specific enhancers such as D2 [Onal et al., 2015], D6 or T1 [Onal et al., 2016a] will be highly useful.

Supplementary Material

Refer to Web version on PubMed Central for supplementary material.

Acknowledgments

We thank members of the Pike Laboratory for the contributions and the members of the UW Biochemistry Animal Support Staff for their contributions to this effort. We would like to thank Charles O'Brien for providing us with the D5−/− mice. We would like to thank Justin J. Jeffery, University of Wisconsin Carbone Cancer Center (UWCCC) Small Animal Imaging Facility and for their help and support.

SOURCES OF FUNDING

This work was supported by NIH grants AR-45173 and DK-74993 to JWP, UWCCC Cancer Center Support Grant P30 CA014520.

References

Al-Aly Z, Shao JS, Lai CF, Huang E, Cai J, Behrmann A, Cheng SL, Towler DA. Aortic Msx2-Wnt calcification cascade is regulated by TNF-alpha-dependent signals in diabetic Ldlr−/− mice. Arterioscler Thromb Vasc Biol. 2007; 27:2589–96. [PubMed: 17932314]

Alexander MR, Owens GK. Epigenetic control of smooth muscle cell differentiation and phenotypic switching in vascular development and disease. Annu Rev Physiol. 2012; 74:13–40. [PubMed: 22017177]

Anderson DM, Maraskovsky E, Billingsley WL, Dougall WC, Tometsko ME, Roux ER, Teepe MC, DuBose RF, Cosman D, Galibert L. A homologue of the TNF receptor and its ligand enhance T-cell growth and dendritic-cell function. Nature. 1997; 390:175–9. [PubMed: 9367155]

Ardeshirpour L, Brian S, Dann P, VanHouten J, Wysolmerski J. Increased PTHrP and decreased estrogens alter bone turnover but do not reproduce the full effects of lactation on the skeleton. Endocrinology. 2010; 151:5591–601. [PubMed: 21047946]

Ardeshirpour L, Dumitru C, Dann P, Sterpka J, VanHouten J, Kim W, Kostenuik P, Wysolmerski J. OPG Treatment Prevents Bone Loss During Lactation But Does Not Affect Milk Production or Maternal Calcium Metabolism. Endocrinology. 2015; 156:2762–73. [PubMed: 25961842]

Bennett BJ, Scatena M, Kirk EA, Rattazzi M, Varon RM, Averill M, Schwartz SM, Giachelli CM, Rosenfeld ME. Osteoprotegerin inactivation accelerates advanced atherosclerotic lesion progression and calcification in older ApoE−/− mice. Arterioscler Thromb Vasc Biol. 2006; 26:2117–24. [PubMed: 16840715]

Bishop KA, Coy HM, Nerenz RD, Meyer MB, Pike JW. Mouse Rankl expression is regulated in T cells by c-Fos through a cluster of distal regulatory enhancers designated the T cell control region. J Biol Chem. 2011; 286:20880–91. [PubMed: 21487009]

Bishop KA, Meyer MB, Pike JW. A novel distal enhancer mediates cytokine induction of mouse RANKl gene expression. Mol Endocrinol. 2009; 23:2095–110. [PubMed: 19880655]

Bishop KA, Wang X, Coy HM, Meyer MB, Gumperz JE, Pike JW. Transcriptional regulation of the human TNFSF11 gene in T cells via a cell type-selective set of distal enhancers. J Cell Biochem. 2015; 116:320–30. [PubMed: 25211367]

Boyle WJ, Simonet WS, Lacey DL. Osteoclast differentiation and activation. Nature. 2003; 423:337–42. [PubMed: 12748652]

Bucay N, Sarosi I, Dunstan CR, Morony S, Tarpley J, Capparelli C, Scully S, Tan HL, Xu W, Lacey DL, Boyle WJ, Simonet WS. osteoprotegerin-deficient mice develop early onset osteoporosis and arterial calcification. Genes Dev. 1998; 12:1260–8. [PubMed: 9573043]

Byon CH, Sun Y, Chen J, Yuan K, Mao X, Heath JM, Anderson PG, Tintut Y, Demer LL, Wang D, Chen Y. Runx2-upregulated receptor activator of nuclear factor κB ligand in calcifying smooth muscle cells promotes migration and osteoclastic differentiation of macrophages. Arterioscler Thromb Vasc Biol. 2011; 31:1387–96. [PubMed: 21454810]

Choi BG, Vilahur G, Cardoso L, Fritton JC, Ibanez B, Zafar MU, Yadegar D, Speidl WS, Schaffler MB, Fuster V, Badimon JJ. Ovariectomy increases vascular calcification via the OPG/RANKL cytokine signalling pathway. Eur J Clin Invest. 2008; 38:211–7. [PubMed: 18279396]

Clowes MM, Lynch CM, Miller AD, Miller DG, Osborne WR, Clowes AW. Long-term biological response of injured rat carotid artery seeded with smooth muscle cells expressing retrovirally introduced human genes. J Clin Invest. 1994; 93:644–51. [PubMed: 8113400]

Collaborators GMaCoD. Global, regional, and national age-sex specific all-cause and cause-specific mortality for 240 causes of death, 1990–2013: a systematic analysis for the Global Burden of Disease Study 2013. Lancet. 2015; 385:117–71. [PubMed: 25530442]

Collin-Osdoby P. Regulation of vascular calcification by osteoclast regulatory factors RANKL and osteoprotegerin. Circ Res. 2004; 95:1046–57. [PubMed: 15564564]

Collin-Osdoby P, Rothe L, Anderson F, Nelson M, Maloney W, Osdoby P. Receptor activator of NF-kappa B and osteoprotegerin expression by human microvascular endothelial cells, regulation by inflammatory cytokines, and role in human osteoclastogenesis. J Biol Chem. 2001; 276:20659–72. [PubMed: 11274143]

Cummings SR, San Martin J, McClung MR, Siris ES, Eastell R, Reid IR, Delmas P, Zoog HB, Austin M, Wang A, Kutilek S, Adami S, Zanchetta J, Libanati C, Siddhanti S, Christiansen C, Trial F. Denosumab for prevention of fractures in postmenopausal women with osteoporosis. N Engl J Med. 2009; 361:756–65. [PubMed: 19671655]

Danks L, Komatsu N, Guerrini MM, Sawa S, Armaka M, Kollias G, Nakashima T, Takayanagi H. RANKL expressed on synovial fibroblasts is primarily responsible for bone erosions during joint inflammation. Ann Rheum Dis. 2015

Deuell KA, Callegari A, Giachelli CM, Rosenfeld ME, Scatena M. RANKL enhances macrophage paracrine pro-calcific activity in high phosphate-treated smooth muscle cells: dependence on IL-6 and TNF-α. J Vasc Res. 2012; 49:510–21. [PubMed: 22948607]

Dhore CR, Cleutjens JP, Lutgens E, Cleutjens KB, Geusens PP, Kitslaar PJ, Tordoir JH, Spronk HM, Vermeer C, Daemen MJ. Differential expression of bone matrix regulatory proteins in human atherosclerotic plaques. Arterioscler Thromb Vasc Biol. 2001; 21:1998–2003. [PubMed: 11742876]

Di Bartolo BA, Cartland SP, Harith HH, Bobryshev YV, Schoppet M, Kavurma MM. TRAIL-deficiency accelerates vascular calcification in atherosclerosis via modulation of RANKL. PLoS One. 2013; 8:e74211. [PubMed: 24040204]

Doherty TM, Asotra K, Fitzpatrick LA, Qiao JH, Wilkin DJ, Detrano RC, Dunstan CR, Shah PK, Rajavashisth TB. Calcification in atherosclerosis: bone biology and chronic inflammation at the arterial crossroads. Proc Natl Acad Sci U S A. 2003; 100:11201–6. [PubMed: 14500910]

Dougall WC, Glaccum M, Charrier K, Rohrbach K, Brasel K, De Smedt T, Daro E, Smith J, Tometsko ME, Maliszewski CR, Armstrong A, Shen V, Bain S, Cosman D, Anderson D, Morrissey PJ, Peschon JJ, Schuh J. RANK is essential for osteoclast and lymph node development. Genes Dev. 1999; 13:2412–24. [PubMed: 10500098]

Fata J, Kong Y, Li J, Sasaki T, Irie-Sasaki J, Moorehead R, Elliott R, Scully S, Voura E, Lacey D, Boyle W, Khokha R, Penninger J. The osteoclast differentiation factor osteoprotegerin-ligand is essential for mammary gland development. Cell. 2000; 103:41–50. [PubMed: 11051546]

Fu Q, Manolagas S, O'Brien C. Parathyroid hormone controls receptor activator of NF-kappaB ligand gene expression via a distant transcriptional enhancer. Mol Cell Biol. 2006; 26:6453–68. [PubMed: 16914731]

Galli C, Zella LA, Fretz JA, Fu Q, Pike JW, Weinstein RS, Manolagas SC, O'Brien CA. Targeted deletion of a distant transcriptional enhancer of the receptor activator of nuclear factor-kappaB ligand gene reduces bone remodeling and increases bone mass. Endocrinology. 2008; 149:146–53. [PubMed: 17932217]

Giachelli CM. Vascular calcification mechanisms. J Am Soc Nephrol. 2004; 15:2959–64. [PubMed: 15579497]

Giachelli CM. The emerging role of phosphate in vascular calcification. Kidney Int. 2009; 75:890–7. [PubMed: 19145240]

Glass CK, Witztum JL. Atherosclerosis. the road ahead. Cell. 2001; 104:503–16. [PubMed: 11239408]

Gu L, Okada Y, Clinton SK, Gerard C, Sukhova GK, Libby P, Rollins BJ. Absence of monocyte chemoattractant protein-1 reduces atherosclerosis in low density lipoprotein receptor-deficient mice. Mol Cell. 1998; 2:275–81. [PubMed: 9734366]

Guerrini MM, Okamoto K, Komatsu N, Sawa S, Danks L, Penninger JM, Nakashima T, Takayanagi H. Inhibition of the TNF Family Cytokine RANKL Prevents Autoimmune Inflammation in the Central Nervous System. Immunity. 2015; 43:1174–85. [PubMed: 26680207]

Guerrini MM, Takayanagi H. The immune system, bone and RANKL. Arch Biochem Biophys. 2014; 561:118–23. [PubMed: 24929185]

Hanada R, Leibbrandt A, Hanada T, Kitaoka S, Furuyashiki T, Fujihara H, Trichereau J, Paolino M, Qadri F, Plehm R, Klaere S, Komnenovic V, Mimata H, Yoshimatsu H, Takahashi N, von Haeseler A, Bader M, Kilic SS, Ueta Y, Pifl C, Narumiya S, Penninger JM. Central control of fever and female body temperature by RANKL/RANK. Nature. 2009; 462:505–9. [PubMed: 19940926]

Hansson GK. Inflammation, atherosclerosis, and coronary artery disease. N Engl J Med. 2005; 352:1685–95. [PubMed: 15843671]

Helas S, Goettsch C, Schoppet M, Zeitz U, Hempel U, Morawietz H, Kostenuik PJ, Erben RG, Hofbauer LC. Inhibition of receptor activator of NF-kappaB ligand by denosumab attenuates vascular calcium deposition in mice. Am J Pathol. 2009; 175:473–8. [PubMed: 19590040]

Hess E, Duheron V, Decossas M, Lézot F, Berdal A, Chea S, Golub R, Bosisio MR, Bridal SL, Choi Y, Yagita H, Mueller CG. RANKL induces organized lymph node growth by stromal cell proliferation. J Immunol. 2012; 188:1245–54. [PubMed: 22210913]

Hofbauer LC, Schoppet M. Osteoprotegerin: a link between osteoporosis and arterial calcification? Lancet. 2001; 358:257–9. [PubMed: 11498208]

Hofbauer LC, Schoppet M. Clinical implications of the osteoprotegerin/RANKL/RANK system for bone and vascular diseases. JAMA. 2004; 292:490–5. [PubMed: 15280347]

Hsu JJ, Tintut Y, Demer LL. Vitamin D and osteogenic differentiation in the artery wall. Clin J Am Soc Nephrol. 2008; 3:1542–7. [PubMed: 18562594]

Hunt JL, Fairman R, Mitchell ME, Carpenter JP, Golden M, Khalapyan T, Wolfe M, Neschis D, Milner R, Scoll B, Cusack A, Mohler ER. Bone formation in carotid plaques: a clinicopathological study. Stroke. 2002; 33:1214–9. [PubMed: 11988593]

Kaden JJ, Bickelhaupt S, Grobholz R, Haase KK, Sarikoç A, Kiliç R, Brueckmann M, Lang S, Zahn I, Vahl C, Hagl S, Dempfle CE, Borggrefe M. Receptor activator of nuclear factor kappaB ligand and osteoprotegerin regulate aortic valve calcification. J Mol Cell Cardiol. 2004; 36:57–66. [PubMed: 14734048]

Kanematsu M, Sato T, Takai H, Watanabe K, Ikeda K, Yamada Y. Prostaglandin E2 induces expression of receptor activator of nuclear factor-kappa B ligand/osteoprotegrin ligand on pre-B cells: implications for accelerated osteoclastogenesis in estrogen deficiency. J Bone Miner Res. 2000; 15:1321–9. [PubMed: 10893680]

Khosla S. The bone and beyond: a shift in calcium. Nat Med. 2011; 17:430–1. [PubMed: 21475237]

Kiechl S, Schett G, Schwaiger J, Seppi K, Eder P, Egger G, Santer P, Mayr A, Xu Q, Willeit J. Soluble receptor activator of nuclear factor-kappa B ligand and risk for cardiovascular disease. Circulation. 2007; 116:385–91. [PubMed: 17620507]

Kiechl S, Wittmann J, Giaccari A, Knoflach M, Willeit P, Bozec A, Moschen AR, Muscogiuri G, Sorice GP, Kireva T, Summerer M, Wirtz S, Luther J, Mielenz D, Billmeier U, Egger G, Mayr A, Oberhollenzer F, Kronenberg F, Orthofer M, Penninger JM, Meigs JB, Bonora E, Tilg H, Willeit J, Schett G. Blockade of receptor activator of nuclear factor-κB (RANKL) signaling improves hepatic insulin resistance and prevents development of diabetes mellitus. Nat Med. 2013; 19:358–63. [PubMed: 23396210]

Kiel DP, Kauppila LI, Cupples LA, Hannan MT, O'Donnell CJ, Wilson PW. Bone loss and the progression of abdominal aortic calcification over a 25 year period: the Framingham Heart Study. Calcif Tissue Int. 2001; 68:271–6. [PubMed: 11683533]

Kim N, Odgren PR, Kim DK, Marks SC, Choi Y. Diverse roles of the tumor necrosis factor family member TRANCE in skeletal physiology revealed by TRANCE deficiency and partial rescue by a lymphocyte-expressed TRANCE transgene. Proc Natl Acad Sci U S A. 2000; 97:10905–10. [PubMed: 10984520]

Kim S, Yamazaki M, Zella L, Shevde N, Pike J. Activation of receptor activator of NF-kappaB ligand gene expression by 1,25-dihydroxyvitamin D3 is mediated through multiple long-range enhancers. Mol Cell Biol. 2006; 26:6469–86. [PubMed: 16914732]

Kong YY, Feige U, Sarosi I, Bolon B, Tafuri A, Morony S, Capparelli C, Li J, Elliott R, McCabe S, Wong T, Campagnuolo G, Moran E, Bogoch ER, Van G, Nguyen LT, Ohashi PS, Lacey DL, Fish E, Boyle WJ, Penninger JM. Activated T cells regulate bone loss and joint destruction in adjuvant arthritis through osteoprotegerin ligand. Nature. 1999a; 402:304–9. [PubMed: 10580503]

Kong YY, Yoshida H, Sarosi I, Tan HL, Timms E, Capparelli C, Morony S, Oliveira-dos-Santos AJ, Van G, Itie A, Khoo W, Wakeham A, Dunstan CR, Lacey DL, Mak TW, Boyle WJ, Penninger JM. OPGL is a key regulator of osteoclastogenesis, lymphocyte development and lymph-node organogenesis. Nature. 1999b; 397:315–23. [PubMed: 9950424]

Lacey DL, Timms E, Tan HL, Kelley MJ, Dunstan CR, Burgess T, Elliott R, Colombero A, Elliott G, Scully S, Hsu H, Sullivan J, Hawkins N, Davy E, Capparelli C, Eli A, Qian YX, Kaufman S, Sarosi I, Shalhoub V, Senaldi G, Guo J, Delaney J, Boyle WJ. Osteoprotegerin ligand is a cytokine that regulates osteoclast differentiation and activation. Cell. 1998; 93:165–76. [PubMed: 9568710]

Lee SM, Bishop KA, Goellner JJ, O'Brien CA, Pike JW. Mouse and Human BAC Transgenes Recapitulate Tissue-Specific Expression of the Vitamin D Receptor in Mice and Rescue the VDR-Null Phenotype. Endocrinology. 2014; 155:2064–76. [PubMed: 24693968]

Libby P. Inflammation in atherosclerosis. Nature. 2002; 420:868–74. [PubMed: 12490960]

Libby P. Mechanisms of acute coronary syndromes and their implications for therapy. N Engl J Med. 2013; 368:2004–13. [PubMed: 23697515]

Libby P, Ridker PM, Hansson GK. Progress and challenges in translating the biology of atherosclerosis. Nature. 2011; 473:317–25. [PubMed: 21593864]

London GM. Arterial calcification: cardiovascular function and clinical outcome. Nefrologia. 2011a; 31:644–7. [PubMed: 22130278]

London GM. Soft bone - hard arteries: a link? Kidney Blood Press Res. 2011b; 34:203–8. [PubMed: 21691122]

Loser K, Mehling A, Loeser S, Apelt J, Kuhn A, Grabbe S, Schwarz T, Penninger JM, Beissert S. Epidermal RANKL controls regulatory T-cell numbers via activation of dendritic cells. Nat Med. 2006; 12:1372–9. [PubMed: 17143276]

Luo J, Yang Z, Ma Y, Yue Z, Lin H, Qu G, Huang J, Dai W, Li C, Zheng C, Xu L, Chen H, Wang J, Li D, Siwko S, Penninger JM, Ning G, Xiao J, Liu M. LGR4 is a receptor for RANKL and negatively regulates osteoclast differentiation and bone resorption. Nat Med. 2016; 22:539–46. [PubMed: 27064449]

McClelland RL, Chung H, Detrano R, Post W, Kronmal RA. Distribution of coronary artery calcium by race, gender, and age: results from the Multi-Ethnic Study of Atherosclerosis (MESA). Circulation. 2006; 113:30–7. [PubMed: 16365194]

Meyer MB, Benkusky NA, Pike JW. The RUNX2 cistrome in osteoblasts: characterization, down-regulation following differentiation, and relationship to gene expression. J Biol Chem. 2014; 289:16016–31. [PubMed: 24764292]

Min H, Morony S, Sarosi I, Dunstan CR, Capparelli C, Scully S, Van G, Kaufman S, Kostenuik PJ, Lacey DL, Boyle WJ, Simonet WS. Osteoprotegerin reverses osteoporosis by inhibiting endosteal osteoclasts and prevents vascular calcification by blocking a process resembling osteoclastogenesis. J Exp Med. 2000; 192:463–74. [PubMed: 10952716]

Mohler ER. Are atherosclerotic processes involved in aortic-valve calcification? Lancet. 2000; 356:524–5. [PubMed: 10950224]

Morony S, Sage AP, Corbin T, Lu J, Tintut Y, Demer LL. Enhanced mineralization potential of vascular cells from SM22α-Rankl (tg) mice. Calcif Tissue Int. 2012; 91:379–86. [PubMed: 23052229]

Naik V, Leaf EM, Hu JH, Yang HY, Nguyen NB, Giachelli CM, Speer MY. Sources of cells that contribute to atherosclerotic intimal calcification: an in vivo genetic fate mapping study. Cardiovasc Res. 2012; 94:545–54. [PubMed: 22436847]

Ndip A, Williams A, Jude EB, Serracino-Inglott F, Richardson S, Smyth JV, Boulton AJ, Alexander MY. The RANKL/RANK/OPG signaling pathway mediates medial arterial calcification in diabetic Charcot neuroarthropathy. Diabetes. 2011; 60:2187–96. [PubMed: 21659498]

Nerenz RD, Martowicz ML, Pike JW. An enhancer 20 kilobases upstream of the human receptor activator of nuclear factor-kappaB ligand gene mediates dominant activation by 1,25-dihydroxyvitamin D3. Mol Endocrinol. 2008; 22:1044–56. [PubMed: 18202151]

O'Brien CA. Control of RANKL gene expression. Bone. 2010; 46:911–9. [PubMed: 19716455]

Olesen M, Skov V, Mechta M, Mumm BH, Rasmussen LM. No influence of OPG and its ligands, RANKL and TRAIL, on proliferation and regulation of the calcification process in primary human vascular smooth muscle cells. Mol Cell Endocrinol. 2012; 362:149–56. [PubMed: 22698523]

Onal M, Bishop KA, St John HC, Danielson AL, Riley EM, Piemontese M, Xiong J, Goellner JJ, O'Brien CA, Pike JW. A DNA Segment Spanning the Mouse Tnfsf11 Transcription Unit and Its Upstream Regulatory Domain Rescues the Pleiotropic Biologic Phenotype of the RANKL Null Mouse. J Bone Miner Res. 2014a; 30:855–68.

Onal M, Galli C, Fu Q, Xiong J, Weinstein RS, Manolagas SC, O'Brien CA. The RANKL distal control region is required for the increase in RANKL expression, but not the bone loss, associated with hyperparathyroidism or lactation in adult mice. Mol Endocrinol. 2012; 26:341–8. [PubMed: 22207718]

Onal M, St John H, Danielson A, O'Brien CA, Pike JW. Unique Distal Enhancers Linked to the Mouse *Tnfsf11* Gene Direct Tissue-Specific Expression and Inflammation induced Regulation of RANKL Expression. J Bone Miner Res. 2014b; 29(Suppl 1) editor^editors.

Onal M, St John HC, Danielson AL, Markert JW, Riley EM, Pike JW. Unique Distal Enhancers Linked to the Mouse Tnfsf11 Gene Direct Tissue-Specific and Inflammation-Induced Expression of RANKL. Endocrinology. 2016a; 157:482–96. [PubMed: 26646205]

Onal M, St John HC, Danielson AL, Pike JW. Deletion of the Distal Tnfsf11 RL-D2 Enhancer that Contributes to PTH-Mediated RANKL Expression in Osteoblast Lineage Cells Results in a High Bone Mass Phenotype in Mice. J Bone Miner Res. 2015

Onal M, St John HC, Danielson AL, Pike JW. Deletion of the Distal Tnfsf11 RL-D2 Enhancer That Contributes to PTH-Mediated RANKL Expression in Osteoblast Lineage Cells Results in a High Bone Mass Phenotype in Mice. J Bone Miner Res. 2016b; 31:416–29. [PubMed: 26332516]

Osako MK, Nakagami H, Koibuchi N, Shimizu H, Nakagami F, Koriyama H, Shimamura M, Miyake T, Rakugi H, Morishita R. Estrogen inhibits vascular calcification via vascular RANKL system: common mechanism of osteoporosis and vascular calcification. Circ Res. 2010; 107:466–75. [PubMed: 20595654]

Panizo S, Cardus A, Encinas M, Parisi E, Valcheva P, López-Ongil S, Coll B, Fernandez E, Valdivielso JM. RANKL increases vascular smooth muscle cell calcification through a RANK-BMP4-dependent pathway. Circ Res. 2009; 104:1041–8. [PubMed: 19325147]

Papadopouli AE, Klonaris CN, Theocharis SE. Role of OPG/RANKL/RANK axis on the vasculature. Histol Histopathol. 2008; 23:497–506. [PubMed: 18228207]

Plump AS, Smith JD, Hayek T, Aalto-Setälä K, Walsh A, Verstuyft JG, Rubin EM, Breslow JL. Severe hypercholesterolemia and atherosclerosis in apolipoprotein E-deficient mice created by homologous recombination in ES cells. Cell. 1992; 71:343–53. [PubMed: 1423598]

Quercioli A, Luciano Viviani G, Dallegri F, Mach F, Montecucco F. Receptor activator of nuclear factor kappa B ligand/osteoprotegerin pathway is a promising target to reduce atherosclerotic plaque calcification. Crit Pathw Cardiol. 2010; 9:227–30. [PubMed: 21119343]

Ross R. Atherosclerosis--an inflammatory disease. N Engl J Med. 1999; 340:115–26. [PubMed: 9887164]

Roth GA, Huffman MD, Moran AE, Feigin V, Mensah GA, Naghavi M, Murray CJ. Global and regional patterns in cardiovascular mortality from 1990 to 2013. Circulation. 2015; 132:1667–78. [PubMed: 26503749]

Sage AP, Tintut Y, Demer LL. Regulatory mechanisms in vascular calcification. Nat Rev Cardiol. 2010; 7:528–36. [PubMed: 20664518]

Sandberg WJ, Yndestad A, Øie E, Smith C, Ueland T, Ovchinnikova O, Robertson AK, Müller F, Semb AG, Scholz H, Andreassen AK, Gullestad L, Damås JK, Frøland SS, Hansson GK, Halvorsen B, Aukrust P. Enhanced T-cell expression of RANK ligand in acute coronary syndrome: possible role in plaque destabilization. Arterioscler Thromb Vasc Biol. 2006; 26:857–63. [PubMed: 16424351]

Schoppet M, Al-Fakhri N, Franke FE, Katz N, Barth PJ, Maisch B, Preissner KT, Hofbauer LC. Localization of osteoprotegerin, tumor necrosis factor-related apoptosis-inducing ligand, and receptor activator of nuclear factor-kappaB ligand in Mönckeberg's sclerosis and atherosclerosis. J Clin Endocrinol Metab. 2004; 89:4104–12. [PubMed: 15292354]

Shamsuzzaman S, Onal M, St John HC, Jeffery JJ, Pike JW. Absence of the Vitamin D Receptor Inhibits Atherosclerotic Plaque Calcification in Female Hypercholesterolemic Mice. J Cell Biochem. 2016

Shanahan CM, Crouthamel MH, Kapustin A, Giachelli CM. Arterial calcification in chronic kidney disease: key roles for calcium and phosphate. Circ Res. 2011; 109:697–711. [PubMed: 21885837]

Shao JS, Cheng SL, Sadhu J, Towler DA. Inflammation and the osteogenic regulation of vascular calcification: a review and perspective. Hypertension. 2010; 55:579–92. [PubMed: 20101002]

Shroff RC, Shanahan CM. The vascular biology of calcification. Semin Dial. 2007; 20:103–9. [PubMed: 17374082]

Simonet WS, Lacey DL, Dunstan CR, Kelley M, Chang MS, Luthy R, Nguyen HQ, Wooden S, Bennett L, Boone T, Shimamoto G, DeRose M, Elliott R, Colombero A, Tan HL, Trail G, Sullivan J, Davy E, Bucay N, Renshaw-Gegg L, Hughes TM, Hill D, Pattison W, Campbell P, Sander S, Van G, Tarpley J, Derby P, Lee R, Boyle WJ. Osteoprotegerin: a novel secreted protein involved in the regulation of bone density. Cell. 1997; 89:309–19. [PubMed: 9108485]

Smith MR, Egerdie B, Hernández Toriz N, Feldman R, Tammela TL, Saad F, Heracek J, Szwedowski M, Ke C, Kupic A, Leder BZ, Goessl C. Group DHPCS. Denosumab in men receiving androgen-deprivation therapy for prostate cancer. N Engl J Med. 2009; 361:745–55. [PubMed: 19671656]

Sobacchi C, Frattini A, Guerrini MM, Abinun M, Pangrazio A, Susani L, Bredius R, Mancini G, Cant A, Bishop N, Grabowski P, Del Fattore A, Messina C, Errigo G, Coxon FP, Scott DI, Teti A, Rogers MJ, Vezzoni P, Villa A, Helfrich MH. Osteoclast-poor human osteopetrosis due to mutations in the gene encoding RANKL. Nat Genet. 2007; 39:960–2. [PubMed: 17632511]

Speer MY, Yang HY, Brabb T, Leaf E, Look A, Lin WL, Frutkin A, Dichek D, Giachelli CM. Smooth muscle cells give rise to osteochondrogenic precursors and chondrocytes in calcifying arteries. Circ Res. 2009; 104:733–41. [PubMed: 19197075]

Steitz SA, Speer MY, Curinga G, Yang HY, Haynes P, Aebersold R, Schinke T, Karsenty G, Giachelli CM. Smooth muscle cell phenotypic transition associated with calcification: upregulation of Cbfa1 and downregulation of smooth muscle lineage markers. Circ Res. 2001; 89:1147–54. [PubMed: 11739279]

Suda T, Takahashi N, Martin TJ. Modulation of osteoclast differentiation. Endocr Rev. 1992; 13:66–80. [PubMed: 1555533]

Sun Y, Byon CH, Yuan K, Chen J, Mao X, Heath JM, Javed A, Zhang K, Anderson PG, Chen Y. Smooth muscle cell-specific runx2 deficiency inhibits vascular calcification. Circ Res. 2012; 111:543–52. [PubMed: 22773442]

Teitelbaum SL. Bone resorption by osteoclasts. Science. 2000; 289:1504–8. [PubMed: 10968780]

Thompson B, Towler DA. Arterial calcification and bone physiology: role of the bone-vascular axis. Nat Rev Endocrinol. 2012; 8:529–43. [PubMed: 22473330]

Tintut Y, Demer L. Role of osteoprotegerin and its ligands and competing receptors in atherosclerotic calcification. J Investig Med. 2006; 54:395–401.

Towler DA. Vascular calcification in ESRD: Another cloud appears in the perfect storm--but highlights a silver lining? Kidney Int. 2004; 66:2467–8. [PubMed: 15569340]

Tseng W, Graham LS, Geng Y, Reddy A, Lu J, Effros RB, Demer L, Tintut Y. PKA-induced receptor activator of NF-kappaB ligand (RANKL) expression in vascular cells mediates osteoclastogenesis but not matrix calcification. J Biol Chem. 2010; 285:29925–31. [PubMed: 20663885]

Wong BR, Rho J, Arron J, Robinson E, Orlinick J, Chao M, Kalachikov S, Cayani E, Bartlett FS 3rd, Frankel WN, Lee SY, Choi Y. TRANCE is a novel ligand of the tumor necrosis factor receptor family that activates c-Jun N-terminal kinase in T cells. J Biol Chem. 1997; 272:25190–4. [PubMed: 9312132]

Xiong J, Onal M, Jilka RL, Weinstein RS, Manolagas SC, O'Brien CA. Matrix-embedded cells control osteoclast formation. Nat Med. 2011; 17:1235–41. [PubMed: 21909103]

Yasuda H, Shima N, Nakagawa N, Yamaguchi K, Kinosaki M, Mochizuki S, Tomoyasu A, Yano K, Goto M, Murakami A, Tsuda E, Morinaga T, Higashio K, Udagawa N, Takahashi N, Suda T. Osteoclast differentiation factor is a ligand for osteoprotegerin/osteoclastogenesis-inhibitory factor and is identical to TRANCE/RANKL. Proc Natl Acad Sci U S A. 1998; 95:3597–602. [PubMed: 9520411]

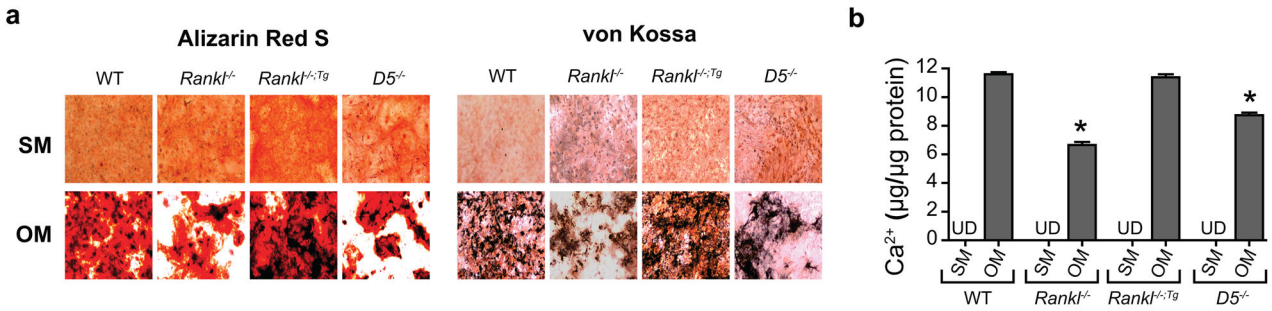

Figure 1. Deletion of the *RANKL* D5 enhancer reduces matrix calcification in murine aortic smooth muscle cells

(a) Murine aortic smooth muscle cells (mAoSMCs) isolated from wild-type (WT), *Rankl*-null ($Rank^{-/-}$), *Rankl* transgenic ($Rankl^{-/-;Tg}$) and D5 enhancer-null ($D5^{-/-}$) mice were differentiated in either standard medium (SM) or osteogenic medium (OM) for 21 days. Alizarin red S and von Kossa staining were carried out to identify deposited calcium in cell layers following differentiation. (b) Calcium content was quantified by decalcifying the cells with 0.6N HCl. $^{*}P < 0.05$ versus SM; Student's *t* test. UD, Undetected.

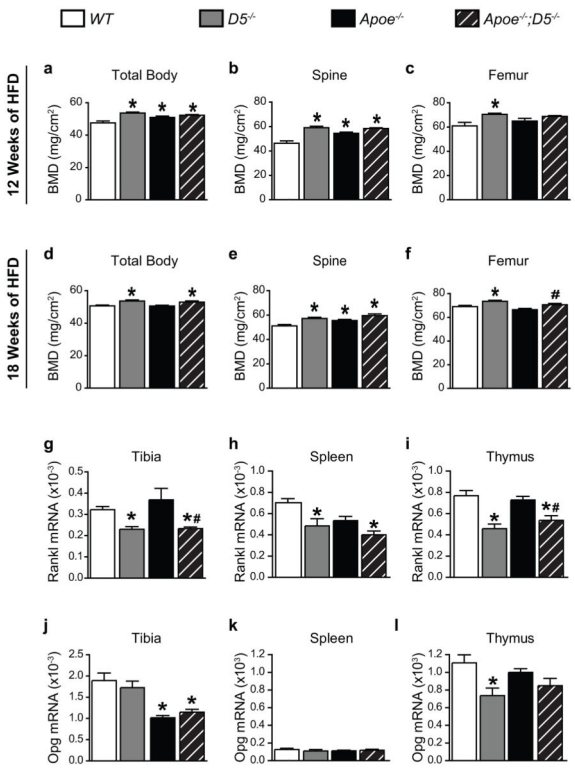

Figure 2. Deletion of the *RANKL* D5 enhancer leads to increased bone mass in hypercholesterolemic *Apoe*-null mice

(a – f), Total body (a and d), lumber spinal (b and e) and femoral (c and f) bone mineral density (BMD) of *WT, D5*$^{-/-}$, *Apoe*$^{-/-}$ and *Apoe*$^{-/-}$*;D5*$^{-/-}$ mice (n = 7 – 10 per group) fed a high-fat diet (HFD) for either 12 or 18 weeks. (g – l), Expression of mRNA transcripts of *Rankl* (g–i) and *Opg* (j–l) in tibiae, spleen and thymus of *WT, D5*$^{-/-}$, *Apoe*$^{-/-}$ and *Apoe*$^{-/-}$*;D5*$^{-/-}$ mice (n = 7 – 10 per group) fed the HFD for 18 weeks, assessed by qRT-PCR and normalized to β-actin. Values represent mean ± s.e.m. $^{*}P < 0.05$ versus WT, $^{\#}P < 0.05$ versus *Apoe*$^{-/-}$, calculated by one-way ANOVA.

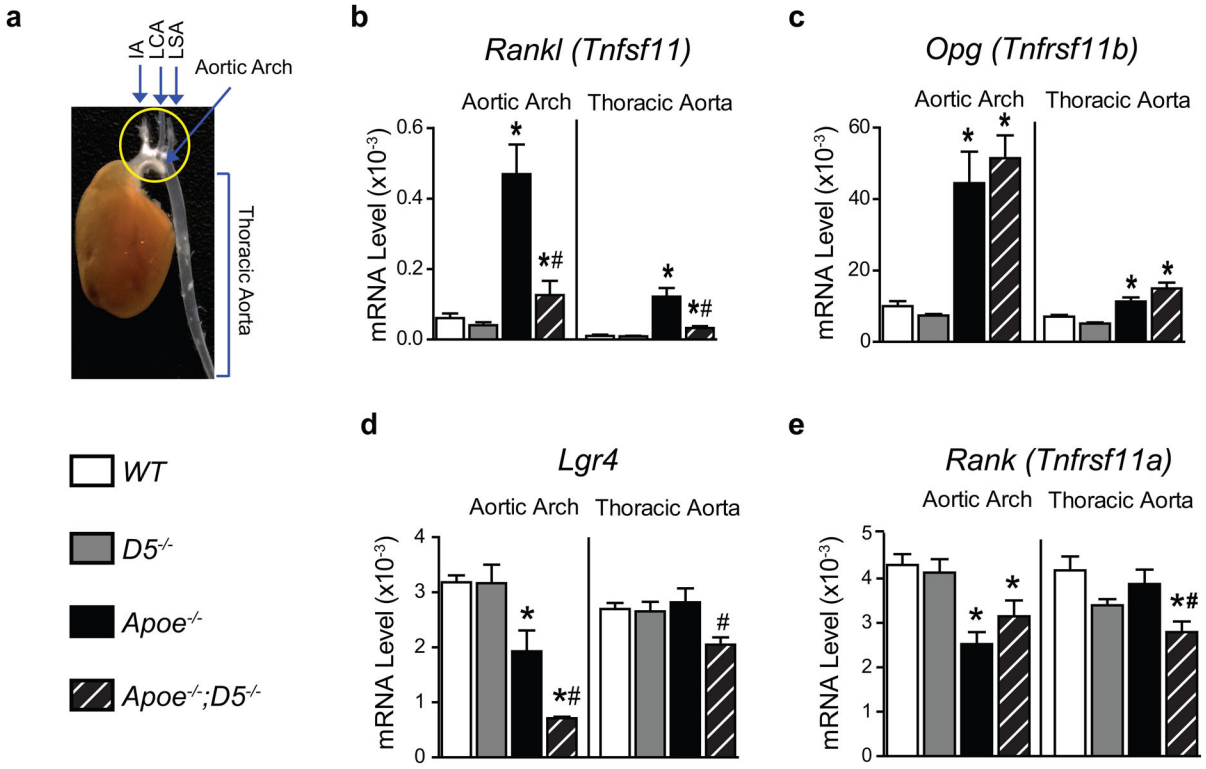

Figure 3. Deletion of the *RANKL* D5 enhancer reduces *RANKL* expression in atherosclerotic lesions

(a) Figure shows a representative picture of an aorta along with the heart that was cleaned off the extra fat and tissues. The aorta was collected after 18 weeks of a high-fat diet (HFD) feeding. The picture shows the aortic arch (circled in yellow) and thoracic aorta. As can be seen, the aortic arch has extensive plaques appears in white fatty streaks whereas few or no fatty streaks are present in the thoracic aorta region. The aortic arches and thoracic aortas were dissected and the RNA was isolated for gene expression analysis. (b – e) Expressions of mRNA transcripts of *Rankl* (b), *Opg* (c), *Lgr4* (d) and *Rank* (e) in the aortic arch and the thoracic aorta of *WT, D5*$^{-/-}$, *Apoe*$^{-/-}$ and *Apoe*$^{-/-}$*;D5*$^{-/-}$ mice (n = 7 – 10 per group) fed the HFD for 18 weeks, assessed by RT-qPCR normalized to β-actin. Values represent mean ± s.e.m. $^{*}P < 0.05$ versus *WT,* $^{\#}P < 0.05$ versus *Apoe*$^{-/-}$, calculated by one-way ANOVA.

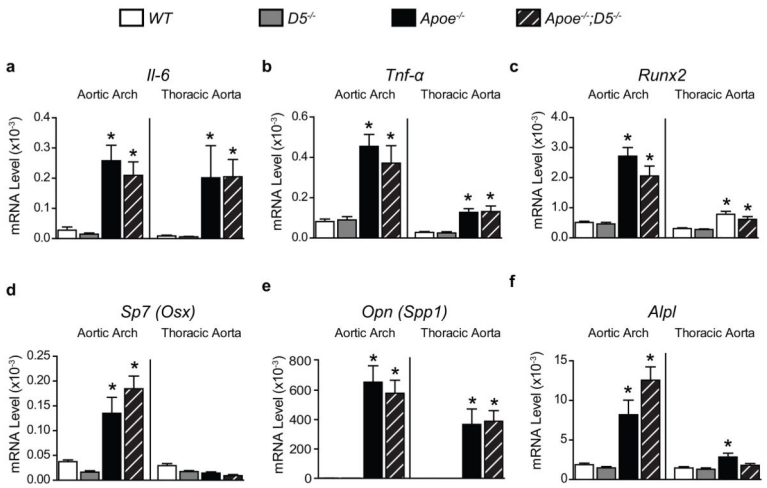

Figure 4. Inflammatory and osteogenic responses are modified in hypercholesterolemic mice

(a – f) Expression of mRNA transcripts of *Il-6* (a), *Tnf-α* (b), *Runx2* (c), *Sp7* (d), *Opn* (e) and *Alpl* (f) in the aortic arch and the thoracic aorta of *WT, D5*$^{-/-}$, *Apoe*$^{-/-}$ and *Apoe*$^{-/-}$*;D5*$^{-/-}$ mice (n = 7 – 10 per group) fed a high-fat diet (HFD) for 18 weeks, assessed by RT-qPCR normalized to β-actin. Values represent mean ± s.e.m. $^{*}P < 0.05$ versus *WT,* $^{\#}P < 0.05$ versus *Apoe*$^{-/-}$, calculated by one-way ANOVA.

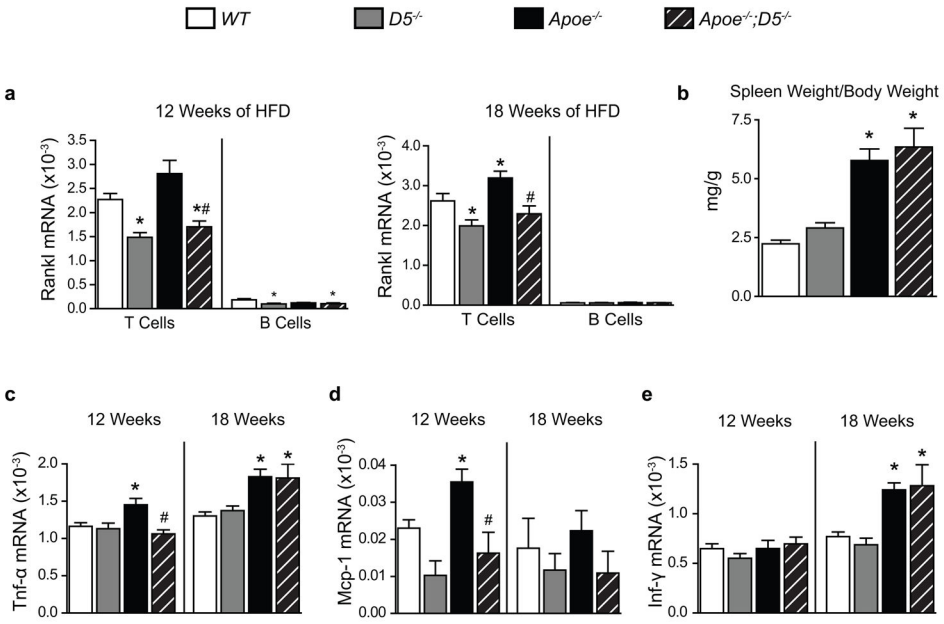

Figure 5. T lymphocyte RANKL increases in atherosclerosis via D5

(a) Expression of *Rankl* mRNA transcripts in splenic pan T and B lymphocytes isolated from *WT, D5*$^{-/-}$, *Apoe*$^{-/-}$ and *Apoe*$^{-/-}$*;D5*$^{-/-}$ mice (n = 7 – 10 per group) fed a high-fat diet (HFD) for either 12 or 18 weeks, assessed by RT-qPCR normalized to β-actin. (b) Splenic weight normalized to total body weight of *WT, D5*$^{-/-}$, *Apoe*$^{-/-}$ and *Apoe*$^{-/-}$*;D5*$^{-/-}$ mice (n = 7 – 10 per group) fed the HFD for 18 weeks. (c – e) Expression of mRNA transcripts of *Tnf-α* (c), *Mcp-1* (d) and *Ifn-γ* (e) in splenic pan T lymphocytes isolated from *WT, D5*$^{-/-}$, *Apoe*$^{-/-}$ and *Apoe*$^{-/-}$*;D5*$^{-/-}$ mice (n = 7 – 10 per group) fed the HFD for either 12 or 18 weeks, assessed by RT-qPCR normalized to β-actin. Values represent mean ± s.e.m. $^{*}P <$ 0.05 versus *WT,* $^{\#}P < 0.05$ versus *Apoe*$^{-/-}$, calculated by one-way ANOVA.

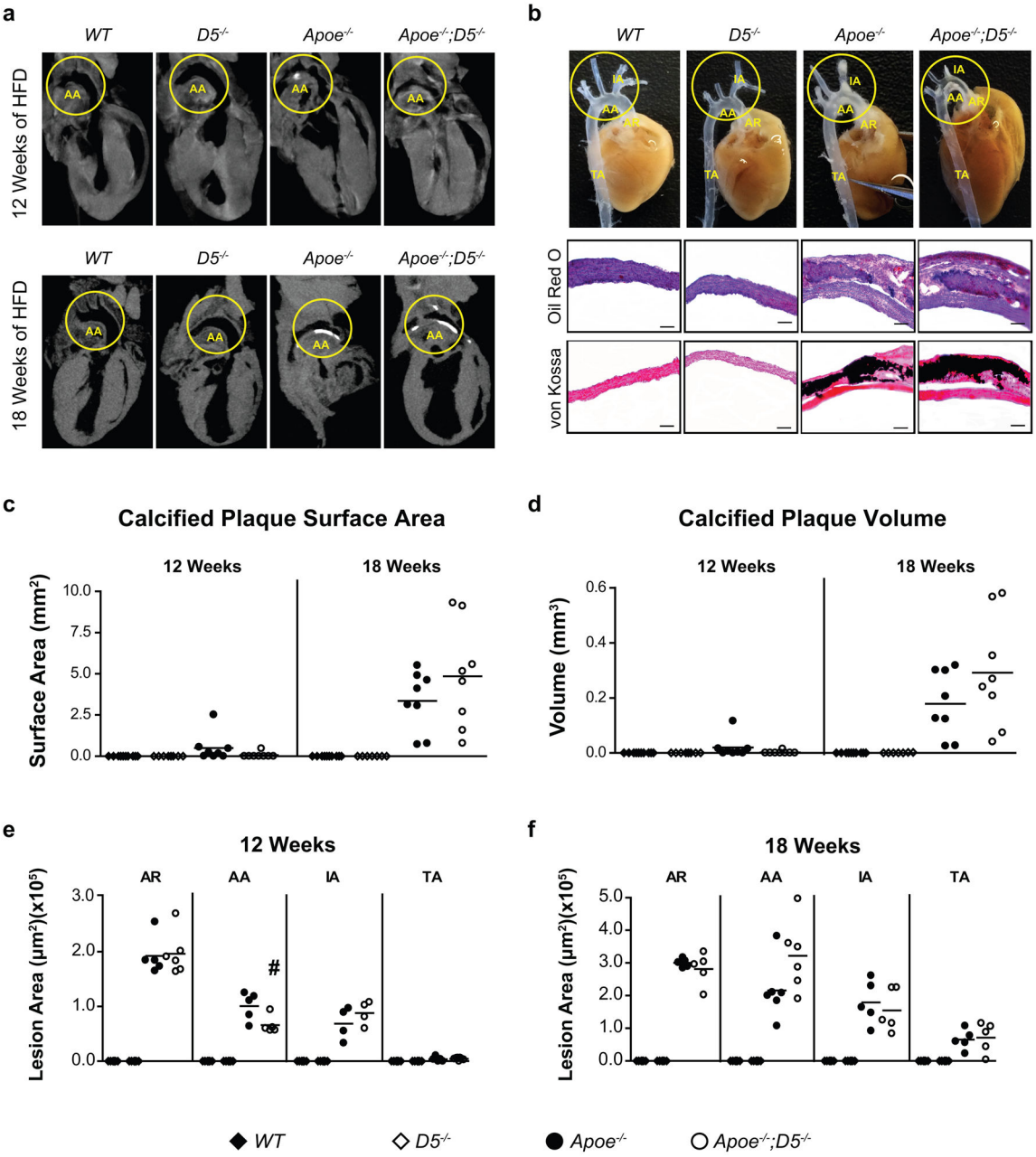

Figure 6. Deletion of the *RANKL* D5 enhancer delays the progression of atherosclerotic plaque formation and plaque calcification in hypercholesterolemic *Apoe*-null mice

(a) Representative µCT images of *WT, D5*$^{-/-}$, *Apoe*$^{-/-}$ and *Apoe*$^{-/-}$*;D5*$^{-/-}$ mice (n = 7 – 10 per group) fed a high-fat diet (HFD) for either 12 or 18 weeks. (b) Representative photographs of aortae showing fatty streaks within aortic root (AR), aortic arch (AA), innominate artery (IA) and thoracic aorta (TA) of *WT, D5*$^{-/-}$, *Apoe*$^{-/-}$ and *Apoe*$^{-/-}$*;D5*$^{-/-}$ mice after 12 weeks of HFD feeding. Oil red O and von Kossa staining confirmed the presence of atherosclerotic lesions and plaque calcification, respectively in the aortic arch of *WT, D5*$^{-/-}$, *Apoe*$^{-/-}$ and *Apoe*$^{-/-}$*;D5*$^{-/-}$ mice after 18 weeks of HFD feeding. Scale bar, 50 µm. (B). (c, d), Total calcified plaque surface area (c) and total calcified plaque volume (d)

quantified by μCT analysis in aortae of *WT, D5*$^{-/-}$, *Apoe*$^{-/-}$ and *Apoe*$^{-/-}$*;D5*$^{-/-}$ mice (n = 5 – 8 per group) fed the HFD for either 12 or 18 weeks. (e, f), Mean atherosclerotic lesion areas in AR, AA, IA and TA of *WT, D5*$^{-/-}$, *Apoe*$^{-/-}$ and *Apoe*$^{-/-}$*;D5*$^{-/-}$ mice (n = 5 – 8 per group) fed the HFD for either 12 or 18 weeks. On scatter plot each point indicates a single mouse. Values represent mean ± s.e.m. $^{*}P < 0.05$ versus *WT*, $^{\#}P < 0.05$ versus *Apoe*$^{-/-}$, calculated by one-way ANOVA.

Table

Frequency of Calcification and Presence of Atherosclerotic Lesions in Aortae.

HFD Feeding	12 Weeks	18 Weeks
Frequency of calcification *		
WT	0% (0/10)	0% (0/10)
D5$^{-/-}$	0% (0/8)	0% (0/7)
Apoe$^{-/-}$	75% (6/8)	100% (8/8)
Apoe$^{-/-}$;*D5*$^{-/-}$	12.5% (1/8)	100% (8/8)
Presence of atherosclerotic lesions †		
WT	0% (0/10)	0% (0/10)
D5$^{-/-}$	0% (0/8)	0% (0/7)
Apoe$^{-/-}$	100% (8/8)	100% (8/8)
Apoe$^{-/-}$;*D5*$^{-/-}$	100% (8/8)	100% (8/8)

*Identified by μCT.

†Identified by oil red O staining.

Numbers in parenthesis indicate number of mice with calcification or atherosclerotic lesions in each group.